

Synthesis of maghemite sub-microspheres by simple solvothermal reduction method

Xian-Ming Liu^{a,b}, Shao-Yun Fu^{a,*}, Hong-Mei Xiao^{a,b}

^a*Technical Institute of Physics and Chemistry, Chinese Academy of Sciences, Beijing 100080, PR China*

^b*Graduate School, Chinese Academy of Sciences, Beijing 100039, PR China*

Received 4 November 2005; received in revised form 10 January 2006; accepted 4 February 2006

Available online 10 March 2006

Abstract

Maghemite sub-micrometer-sized spheres were successfully prepared by a simple solvothermal reduction route at relatively low temperature. The as-obtained sample was characterized by X-ray diffraction (XRD), transmission electron microscopy (TEM), electron diffraction (ED), X-ray photoelectron spectroscopy (XPS) and superconducting quantum interference device (SQUID) measurements. XRD and XPS analyses indicate the formation of γ -Fe₂O₃ phase. TEM results reveal that the γ -Fe₂O₃ particles are spherical with the diameter of 200–400 nm. Magnetic measurements show that the Curie temperature of γ -Fe₂O₃ sub-microspheres is over 400 K and the sample exhibits ferromagnetic behavior at room temperature. It is found that the sub-microspheres possess high saturation magnetization of 81 emu/g at 300 K.

© 2006 Elsevier Inc. All rights reserved.

Keywords: Maghemite; Sub-microsphere; Solvothermal reduction method; Ferromagnetic behavior

1. Introduction

The synthesis of nanostructured magnetic materials has become a particularly important area of research and is attracting a growing interest because of the potential applications such materials have in ferrofluids, advanced magnetic materials, catalysts, colored pigments, high-density magnetic recording media, and medical diagnostics [1–7]. Among a variety of magnetic materials, γ -Fe₂O₃ powders have been widely used for the longest period of time due to their excellent ferromagnetic properties. Maghemite is a ferromagnetic oxide that has been already widely used as magnetic recording materials. Due to the chemical stability, biocompatibility and the heating ability of maghemite nanoparticles in an alternating field, ferrofluids of maghemite nanoparticles can be also used for ferrofluids hyperthermia (MFH) in tumour treatment [8,9]. Previously, maghemite nanoparticles have been prepared by wet chemical methods [10–12]. These methods offer

little control over particle morphology, resulting in these materials with varying quality and magnetic properties. However, most technological applications will require particles with uniform morphology and excellent magnetic properties. In an attempt to gain better processing control over the particle morphology and magnetic properties, the synthesis of monodisperse and size-controlled magnetic ferrite nanoparticles has been reported by several groups. Alivisatos and co-workers synthesized γ -Fe₂O₃ nanoparticles from the direct thermal decomposition of iron cupferron complexes [13]. Hyeon and co-workers reported the synthesis of monodisperse and highly crystalline γ -Fe₂O₃ nanoparticles without the need for a size-selection process [14]. Furthermore, there are several reports on synthesis and characterization of nanostructured maghemite, such as nanoneedles [15], nanorods [16] and nanoplates [17]. Most of these approaches were focused on the synthesis of γ -Fe₂O₃ nanoparticles with a diameter below 100 nm and the preparation process is cumbersome.

For high performance in function-specific biological applications, magnetic particles must be spherical and have smooth surfaces, narrow size distributions, large surface areas (for maximal protein or enzyme binding), high

*Corresponding author. Fax: +86 10 82543752.

E-mail addresses: xiuxm@cl.cryo.ac.cn (X.-M. Liu), syfu@mail.ipc.ac.cn (S.-Y. Fu).

magnetic saturation (M_s) to provide maximum signal, and good dispersion in liquid media [18,19]. Little attention has been paid to the synthesis of monodisperse and micrometer-sized magnetic material spheres. Controlling the size, shape, monodispersity, and yield of the desired product has become a challenge for material chemists. Recently, Li and co-workers developed a solvothermal reduction method to synthesize monodisperse, hydrophilic, and single-crystalline ferrite microspheres with the diameter of 200–800 nm [20]. However, it is noted that microspherical maghemite was obtained by oxidation of the as-synthesized Fe_3O_4 in aqueous solution. To the best of our knowledge, there are no reports on the straightforward synthesis of well-crystallized $\gamma\text{-Fe}_2\text{O}_3$ sub-microspheres. Herein we report a simple approach for the straightforward synthesis of monodisperse maghemite sub-microspheres by a solvothermal reduction method at low temperature. We designed a modified synthetic route in which three added features were found to be critical. Ethylene glycol is only used as solvent in this approach, while formamide is used as a reducing reagent. The reducing reaction of Fe^{3+} ions cannot occur at room temperature using this reducing reagent. Magnetic particles have a strong tendency to agglomerate during their formation in the liquid-phase process. Polyvinylpyrrolidone (PVP) was added as a surfactant and as an additional preventative measure against particle agglomeration. The third feature is that maghemite sub-microspheres can be synthesized in a one-step process.

2. Experimental

2.1. Materials

Chemical reagents such as ethylene glycol (EG), formamide, hydrated iron(III) chloride ($\text{FeCl}_3 \cdot 6\text{H}_2\text{O}$), PVP and hydrazine hydrate ($\text{N}_2\text{H}_4 \cdot \text{H}_2\text{O}$) were supplied from Beijing Chemicals Company of analytical grade and used as received without further purification. Deionized water was used in the experiments.

2.2. Synthesis of maghemite sub-microspheres

The maghemite sub-microspheres were synthesized by hydrothermal treatment using $\text{FeCl}_3 \cdot 6\text{H}_2\text{O}$ as the iron source materials. In a typical experimental procedure, $\text{FeCl}_3 \cdot 6\text{H}_2\text{O}$ (0.5 g) and PVP (0.5 g, MW 58 000) were dissolved in EG (35 mL) and formamide (5 mL, 99%) to form a clear yellow solution. After vigorously stirring for 10 min, the mixture was then transferred into a teflon-lined stainless-steel autoclave with a capacity of 50 mL for hydrothermal treatment at 160 °C for 8 h. After the autoclave had cooled down to room temperature naturally, the precipitates were separated by centrifugation, washed several times with absolute ethanol and deionized water, and subsequently dried under vacuum at 60 °C. At last, a brown product was obtained. As comparative experiments, the above experiments were carried out at 120 and 140 °C,

respectively. Meanwhile, the comparative experiment using $\text{N}_2\text{H}_4 \cdot \text{H}_2\text{O}$ as a reducing reagent was conducted under the same other conditions.

2.3. Characterization

The product was characterized by X-ray power diffraction (XRD) using a Rigaku D/max2500 diffractometer equipped with graphite-monochromated $\text{CuK}\alpha$ radiation ($\lambda = 1.54178 \text{ \AA}$), employing a scanning rate of 0.02 degree/s in the 2θ ranging from 10° to 70°. The transmission electron microscopy (TEM) photographs and the electron diffraction (ED) pattern were recorded on a Hitachi H-800 transmission electron microscope, using an accelerating voltage of 200 kV. X-ray photoelectron spectroscopy (XPS) data were obtained with an ESCALab220i-XL electron spectrometer from VG Scientific using 300 W $\text{AlK}\alpha$ radiation. The base pressure was about 3×10^{-9} mbar. Magnetic studies were carried out on a Quantum Design SQUID magnetometer.

3. Results and discussion

The XRD pattern of the as-prepared product was shown in Fig. 1. The X-ray powder diffraction pattern of the material proved its crystalline nature and the peaks matched well with standard $\gamma\text{-Fe}_2\text{O}_3$ reflections. Although the product was brown, no $\alpha\text{-Fe}_2\text{O}_3$ phase was shown in the XRD pattern of the sample. However, since the XRD patterns of $\gamma\text{-Fe}_2\text{O}_3$ and Fe_3O_4 are very similar, it is difficult to distinguish the two phases simply from XRD patterns. Even so, by comparison with the d values of the experiment and those of standard maghemite (JCPDS card no. 39-1346) and magnetite (JCPDS card no. 19-629) data, it can be found that the results of the experiment are much closer to those of no. 39-1346.

It is known that XRD is not an ideal method to characterize certain crystalline forms of iron-containing nanoparticles, such as $\gamma\text{-Fe}_2\text{O}_3$ (cubic maghemite) and Fe_3O_4 (magnetite), because they both possess the inverse

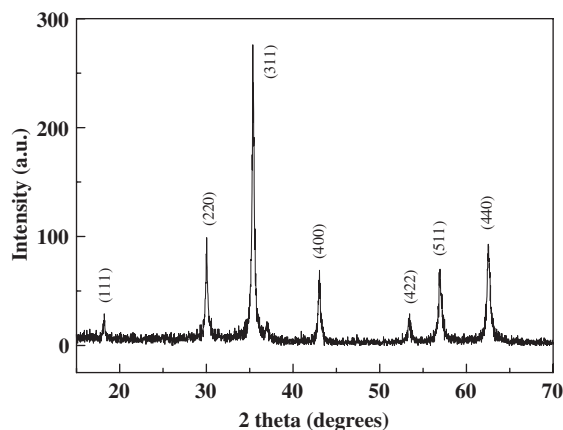


Fig. 1. XRD pattern of maghemite sub-microspheres.

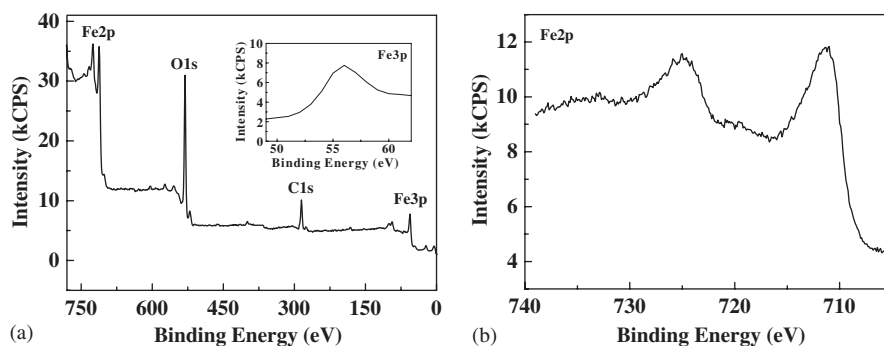


Fig. 2. (a) XPS spectra of maghemite sub-microspheres. Inset is the XPS spectrum of Fe 3*p*. (b) XPS spectrum of Fe 2*p*.

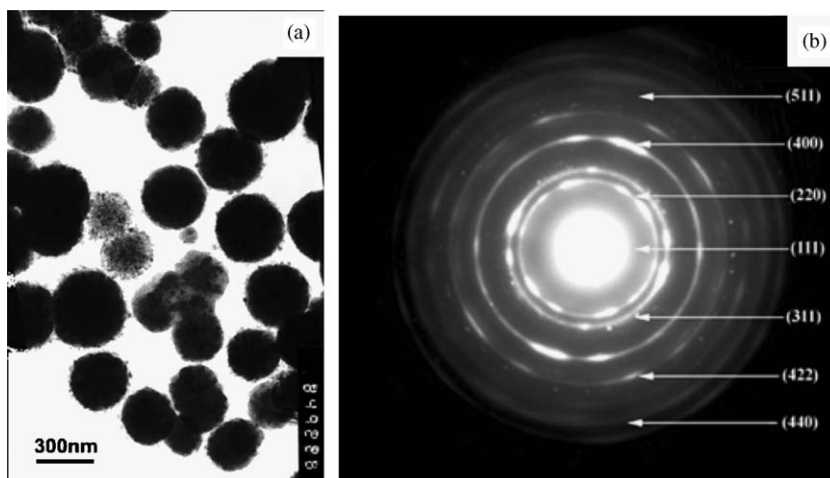


Fig. 3. TEM photograph (a) and ED pattern (b) of the sample.

spinel structure and can have similar XRD patterns as mentioned above. XPS was used to examine shell structure of these nanoparticles, because core electron lines of ferrous and ferric ions can both be detected and distinguishable in XPS. This technique has been used to differentiate between Fe_2O_3 and Fe_3O_4 [21,22]. Fig. 2a showed representative XPS spectra of the product. Elemental analysis confirms the presence of Fe and O elemental signatures. No other metallic iron signals could be detected in the XPS spectra. A relatively weak Fe 3*p* line at 55.9 eV was also detected (inset of Fig. 2a). The photoelectron peaks at 711 and 725 eV are the characteristic doublet of Fe 2*p*_{3/2} and 2*p*_{1/2} core-level spectra of iron oxide, respectively, as shown in Fig. 2b. Both Fe 2*p* and 3*p* data matched closely with those of Fe_2O_3 recorded in the literature [22]. Through calculation of peak area, the atom ratio of Fe and O is about 2:3. It can be obtained that the valences of Fe and O are +3 and –2 in proper orders. The observed XPS spectra of C 1*s* (284.8 eV) and O 1*s* (530.4 eV) come from adventitious carbon and iron oxides.

TEM image of the sample was shown in Fig. 3a. As shown in Fig. 3a, $\gamma\text{-Fe}_2\text{O}_3$ powders consist of sub-microspherical particles. The diameter of a single $\gamma\text{-Fe}_2\text{O}_3$ sub-microsphere can be estimated to be in the range of 200–400 nm. We consider that the morphology of the final

product should be spherical, and this kind of spherical structure was formed only by the self-assembly of $\gamma\text{-Fe}_2\text{O}_3$ nanoparticles. In the meantime, the ED pattern (Fig. 3b) corresponding to bright field images showed that these sub-microspheres consist of $\gamma\text{-Fe}_2\text{O}_3$ nanoparticles with a deficient spinel structure.

A possible formation process of the sub-microspherical $\gamma\text{-Fe}_2\text{O}_3$ particles was suggested according to the designed route. First, Fe^{3+} ions reacted with weak reduction reagent to produce green $\text{Fe}(\text{OH})_2$ together with small amount of black Fe_3O_4 in EG solution by solvothermal treatment. Then, the precipitates were centrifugated and washed using deionized water in the air atmosphere. Since the intermediate products are active, they were quickly oxidized by oxygen when these intermediate products were treated in air. Thus, the sub-microspherical $\gamma\text{-Fe}_2\text{O}_3$ particles were obtained. In order to understand the formation mechanism of maghemite sub-microspheres, it was essential to investigate the influences of some reaction factors such as reaction temperature and the reducing reagent. By varying the experimental conditions, control experiments showed that the yield of maghemite sub-microspheres is very low at 120 or 140 °C. Moreover, when $\text{N}_2\text{H}_4 \cdot \text{H}_2\text{O}$ was used as the reducing reagent, $\gamma\text{-Fe}_2\text{O}_3$ spheres cannot be formed. It can be seen from Fig. 4 that maghemite nanosized particles

together with nanorods were prepared by solvothermal method using $\text{N}_2\text{H}_4 \cdot \text{H}_2\text{O}$ as the reducing reagent. The comparative experimental results indicated that the experimental temperature has a close relation with the maghemite morphologies because the reaction temperature is a key factor affecting the formation of nuclei. On the other hand, the reducing reagent was also very necessary to form complete, stable maghemite sub-microspheres.

Magnetic properties of the sample were derived from zero-field-cooled and field-cooled (ZFC/FC) magnetization as a function of temperature and from magnetization vs magnetic field loops at 300 K, respectively. The sample was initially cooled in a zero field to 2 K. A 10 Oe field was then applied and magnetization was recorded as the temperature was increased (this is a ZFC curve). When the temperature reached 400 K, the sample was progressively

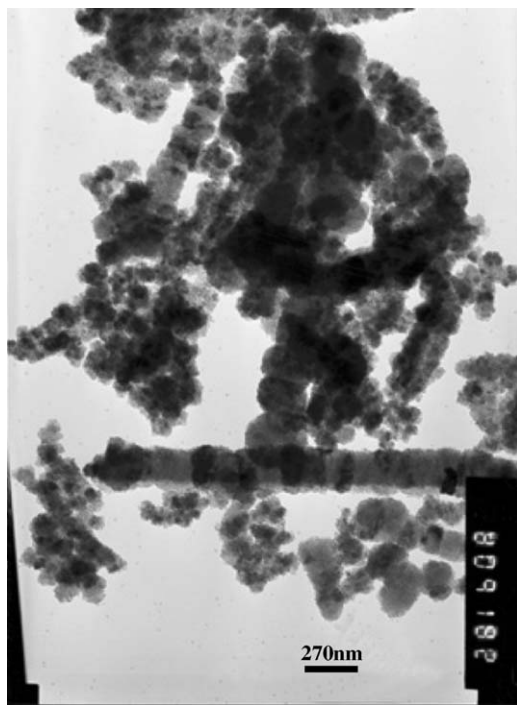


Fig. 4. TEM photograph of $\gamma\text{-Fe}_2\text{O}_3$ nanoparticles together with nanorods prepared by solvothermal method using $\text{N}_2\text{H}_4 \cdot \text{H}_2\text{O}$ as the reducing reagent.

cooled and the magnetization was recorded. This curve is called FC. A complete irreversibility between the curves measured in FC and ZFC modes is observed in Fig. 5(a). In the FC curve, the magnetization nearly stays constant from 400 to 2 K as the temperature decreases. A maximum magnetization cannot be observed in the ZFC curve in the temperature range 2–400 K. The results showed that the Curie temperature is over 400 K and the sample should show ferromagnetic behavior at room temperature. The M – H curve at 300 K, shown in Fig. 5(b), shows a nonlinear, reversible behavior with observed coercivity and remanence (the inset of Fig. 5(b)). At 300 K, a specific saturation magnetization of 81 emu/g is achieved, which is far higher than the reported data in the literature [20]. And the loop still shows a measurable hysteresis even though the coercivity of the product is very small (61 Oe), which is lower than that of plate-shaped $\gamma\text{-Fe}_2\text{O}_3$ nanoparticles [17]. It is suggested that the as-prepared $\gamma\text{-Fe}_2\text{O}_3$ sub-microspheres is self-assembled by $\gamma\text{-Fe}_2\text{O}_3$ nanoparticles and the shape anisotropy is very small, resulting in high magnetization and small coercivity. The magnetization can saturate at low applied field, which indicates that the as-prepared $\gamma\text{-Fe}_2\text{O}_3$ sub-microspheres exhibit a typical ferromagnetic behavior.

4. Conclusions

In summary, maghemite sub-microspheres were successfully synthesized by a simple solvothermal reduction route in a one-step process, and the obtained product could be easily collected and treated. No $\alpha\text{-Fe}_2\text{O}_3$ phase was shown in the XRD pattern of the sample. Although the XRD pattern of Fe_3O_4 is very close to that of $\gamma\text{-Fe}_2\text{O}_3$, XPS spectra proved that the final product was $\gamma\text{-Fe}_2\text{O}_3$. TEM analysis showed that the particle size is controllable, with diameters ranging from 200 to 400 nm. The comparative experimental results indicated that the experimental temperature and the reducing reagent were very necessary to form complete, stable maghemite sub-microspheres. Magnetic characterization demonstrates that sub-microspherical maghemite has a typical ferromagnetic behavior.

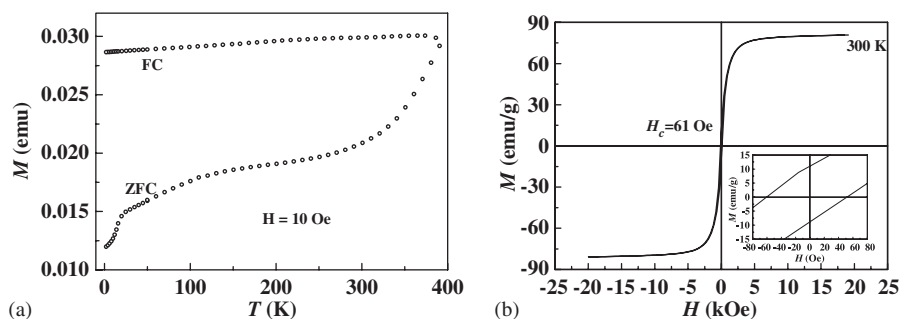


Fig. 5. (a) Temperature-dependent FC and ZFC magnetization measured in the magnetic field of 10 Oe; (b) magnetic hysteresis loops of the sample at 300 K; the inset is an enlarged magnetization curve at low applied fields.

Acknowledgment

We appreciate the financial support of the National High Technical Research and Development Program of China (No. 2003AA305890).

References

- [1] F. Caruso, M. Spasova, A. Susha, M. Giersig, R.A. Caruso, *Chem. Mater.* 13 (2001) 109.
- [2] T. Hyeon, Y. Chung, J. Park, S.S. Lee, Y.W. Kim, B.H. Park, *J. Phys. Chem. B* 106 (2002) 6831.
- [3] Y. Xiong, X. Xie, S. Chen, Z. Li, *Chem. Eur. J.* 9 (2003) 4991.
- [4] K. Woo, H.J. Lee, J. Ahn, Y.S. Park, *Adv. Mater.* 15 (2003) 1761.
- [5] Y. Wang, X. Teng, J. Wang, H. Yang, *Nano. Lett.* 3 (2003) 789.
- [6] A.C.C. Yu, M. Mizuno, Y. Sasaki, H. Kondo, K. Hiraga, *Appl. Phys. Lett.* 81 (2002) 3768.
- [7] X.M. Liu, S.Y. Fu, H.M. Xiao, C.J. Huang, *J. Solid State Chem.* 178 (2005) 2798.
- [8] A. Jordan, R. Scholz, P. Wust, H. Schirra, T. Schiestel, H. Schmidt, R. Felix, *J. Magn. Magn. Mater.* 194 (1999) 185.
- [9] D.C.F. Chan, D.B. Kirpotin, P.A. Bunn Jr., *J. Magn. Magn. Mater.* 122 (1993) 374.
- [10] D. Chen, R. Xu, *J. Solid State Chem.* 137 (1998) 185.
- [11] A. Bee, R. Massart, S. Neveu, *J. Magn. Magn. Mater.* 149 (1995) 6.
- [12] L. Garcell, M.P. Morales, M. Andres-Vergés, P. Tartaj, C.J. Serna, *J. Colloid Interfac. Sci.* 205 (1998) 470.
- [13] J. Rockenberger, E.C. Scher, A.P. Alivisatos, *J. Am. Chem. Soc.* 121 (1999) 11595.
- [14] T. Hyeon, S.S. Lee, J. Park, Y. Chung, H.B. Na, *J. Am. Chem. Soc.* 123 (2001) 12798.
- [15] J. Fang, A. Kumbhar, W.L. Zhou, K.L. Stokes, *Mater. Res. Bull.* 38 (2003) 461.
- [16] V. Chhabra, P. Ayyub, S. Chattopadhyay, A.N. Maitra, *Mater. Lett.* 26 (1996) 21.
- [17] Y. Ni, X. Ge, Z. Zhang, Q. Ye, *Chem. Mater.* 14 (2002) 1048.
- [18] S.H. Gee, Y.K. Hong, D.W. Erickson, M.H. Park, J.C. Sur, *J. Appl. Phys.* 93 (2003) 7560.
- [19] K. Woo, J. Hong, S. Choi, H. Lee, J. Ahn, C.S. Kim, S.W. Lee, *Chem. Mater.* 16 (2004) 2814.
- [20] H. Deng, X. Li, Q. Peng, X. Wang, J. Chen, Y. Li, *Angew. Chem. Int. Ed.* 44 (2005) 2782.
- [21] N.S. McIntyre, D.G. Zetaruk, *Anal. Chem.* 49 (1977) 1521.
- [22] T. Fujii, F.M.F. de Groot, G.A. Sawatzky, F.C. Voogt, T. Hibma, K. Okada, *Phys. Rev. B* 59 (1999) 3195.